

**VIETNAM ACADEMY OF SCIENCE AND TECHNOLOGY
INSTITUTE OF PHYSICS**

**The 8th Academic Conference on Natural Science
for Young Scientists Master & PhD. Students
from ASEAN Countries**

Vinh City, Vietnam. August 27-30, 2023



  **8th ASEAN** 
The 8th Academic Conference on **Natural Science**
for Young Scientists, Master & PhD Students
from ASEAN Countries
August 27-30, 2023
Vinh University, Vinh city, Nghe An province, Viet Nam

PROCEEDINGS



Publishing House for Science and Technology

VIETNAM ACADEMY OF SCIENCE AND TECHNOLOGY
INSTITUTE OF PHYSICS

**THE 8th ACADEMIC CONFERENCE ON
NATURAL SCIENCE FOR YOUNG SCIENTISTS,
MASTER AND PhD STUDENTS
FROM ASEAN COUNTRIES
(CASEAN - 8)**

Vinh City, Vietnam. 27-30 August 2023

PROCEEDINGS

ISBN: 978- 604- 357- 225-4

Publishing House for Science and Technology - 2023

EFFECT OF DRYING MODES ON ANTHOCYANIN CONTENT IN THE PRODUCTION PROCESS OF PURPLE SWEET POTATO POWDER.....	589
Tran Thi Thu Huong, Dinh Thi Hai Thuan	589
CONFINEMENT LOSS CHARACTERISTICS OF SQUARE LATTICE PCFS WITH As₂S₃ SUBSTRATES FOR DIFFERENT NUMBERS OF AIR-HOLE RINGS.....	598
Ngoan Le Thi, Trong Dang Van, Danh Nguyen Thanh, Tan Tran Duy, Thien Nguyen Minh, Luu Mai Van, Bao Le Xuan, Vinh Nguyen Thanh, Lanh Chu Van	598
STUDY ON THE THERMAL DECOMPOSITION PROCESS OF 2,4,6-TRINITRORESORCINOL USING NON-ISOTHERMAL METHODS	604
Trung Huu Hoang, Van Tinh Nguyen, Trung Toan Nguyen.....	604
A STUDY ON THE COMBUSTION CHARACTERISTICS OF KNO₃-BASED MATERIALS CONTAINING PHENOL FORMALDEHYDE RESIN AND SORBITOL	612
Nguyen Duy Tuan, Doan Minh Khai, Nguyen Tuan Anh, Tran Bao Trung, Vu Van Hieu	612
DISPERSION CHARACTERISTICS OF FUSED SILICA GLASS DUAL - CORE PHOTONIC CRYSTAL FIBER.....	619
Phuong Nguyen Thi Hong, Ngoc Vo Thi Minh, Lanh Chu Van, Quang Ho Dinh, Van Nguyen Thi Hai, Mattia Longobucco, Anh Nguyen Lan, Yen Le Thi Hai, Hieu Van Le	619
DEVELOPMENT OF AUTONOMOUS HARVESTING ROBOTS IN THE AGRICULTURE GREENHOUSE ENVIRONMENT BASED ON ROBOT OPERATING SYSTEM	625
Nguyen Thị Duyen, Ngo Manh Tien, Dam Quoc Vuong, Ngo Quang Uoc	625
TEMPERATURE TRANSFORMATION IN FIRE ZONES OF PROPELLANT ON NITRATE CELLULOSE AND NITROGLYCERIN WITH P/H=1.....	632
Pham Quang Hieu, Vu Xuan Son	632
DETERMINATION OF LIQUID PROPERTY BASED ON DYNAMICAL SURFACE REFLECTION.....	639
Dang Khoa Tao, Danh Tien Vu, Le Phuong Hoang, Xuan Binh Cao	639
DESIGN AND IMPLEMENTATION OF A LOW-COST CNC LASER ENGRAVING MACHINE FOR UNIVERSITY LABORATORIES.....	644
Duong Dinh Tu, Mai The Anh, Ho Sy Phuong, Le Van Chuong, Ta Hung Cuong, Vu Van Thanh, Le Thi Thu Uyen.....	644
DESIGN AND IMPLEMENTATION OF REAL-TIME SELF-DRIVING CAR USING CONVOLUTIONAL NEURAL NETWORK AND IOT.....	651
Duong Dinh Tu, Mai The Anh, Ho Sy Phuong, Le Van Chuong, Ta Hung Cuong, Nguyen Xuan Hung, Tran Huy Hoang	651
ELECTROMAGNETICALLY INDUCED GRATING IN A FOUR-LEVEL INVERTED-Y ATOMIC SYSTEM.....	659
Dinh Xuan Khoa, Nguyen Huy Bang, Nguyen Van Phu and Le Van Doai	659

ELECTROMAGNETICALLY INDUCED GRATING IN A FOUR-LEVEL INVERTED-Y ATOMIC SYSTEM

Dinh Xuan Khoa, Nguyen Huy Bang, Nguyen Van Phu and Le Van Doai*

Vinh University, 182 Le Duan Street, Vinh City, Vietnam

*E-mail: doailv@vinhuni.edu.vn

Abstract. In this work, we study the formation of the diffraction pattern of electromagnetically induced grating (EIG) in a four-level inverted-Y atomic system. The influence of laser parameters on diffraction efficiency is also considered. It shows that in the presence of signal laser field, the light energy switching between the zero-, first-, and second-order diffractions can be achieved by tuning frequency and/or intensity of the coupling and signal fields.

Keywords: *Electromagnetically induced transparency; Electromagnetically induced grating; Diffraction grating.*

I. INTRODUCTION

Diffraction grating is commonly used as dispersive elements in many optical systems for applications including spectrometers, switching, tuning and trimming elements in dense wavelength-division multiplexing, visual display technology, external cavity lasers, etc., [1]. The diffraction efficiency of grating is an important parameter since it will strongly influence the final energy delivered by the optical diffraction system.

The coherent interaction between the laser fields with the atom can lead to quantum interference of transition probabilities within the atomic system. The consequence of this quantum interference is to suppress (destructive interference) or enhance (constructive interference) the total transition probability and thus radically change the absorption or transmission property of the atomic medium for a light field. The constructive interference of transition probabilities generates electromagnetically induced transparency (EIT) [2]. Under the EIT condition, the medium forms peculiar optical properties and thus it offers unusual applications such as [3] giant nonlinearity, low threshold optical bistability, and so on.

On the other hand, based on the EIT effect, an atom sample can behave like a diffraction grating which is called an electromagnetically induced grating (EIG) [4]. EIG was first proposed in 1998 [4] and experimentally verified in 1999 [5]. Since then, theoretical and experimental studies of EIG have attracted great attentions [6,7] due to their potential applications in many fields, such as angular Talbot effect [8] and giant Goos-Hänchen shifts [9]. Recently, EIG has been interested in four-level systems with the support of other external fields such as microwave field [10] and magnetic field [11], Kerr nonlinearity [12]. In this work, we study the formation of the diffraction pattern of EIG in a four-level inverted-Y atomic system. The influence of laser parameters on diffraction efficiency is also considered.

II. THEORETICAL MODEL

We consider the interaction of three light fields with a four-level inverted-Y atomic system as shown in Fig. 1a. A weak probe laser beam (with frequency ω_p and Rabi frequency

Ω_p) applies to the transition $|1\rangle \leftrightarrow |3\rangle$, an intense standing-wave coupling field (with frequency ω_c and Rabi frequency Ω_c) couples the transition $|3\rangle \leftrightarrow |4\rangle$, and a weak signal laser beam (with frequency ω_s and Rabi frequency Ω_s) drives the transition $|2\rangle \leftrightarrow |3\rangle$. In experiment, the forward and backward components of the standing-wave coupling field are formed along the x -direction, and the probe and signal fields enters the medium in the z -direction, as shown in Fig. 1b.

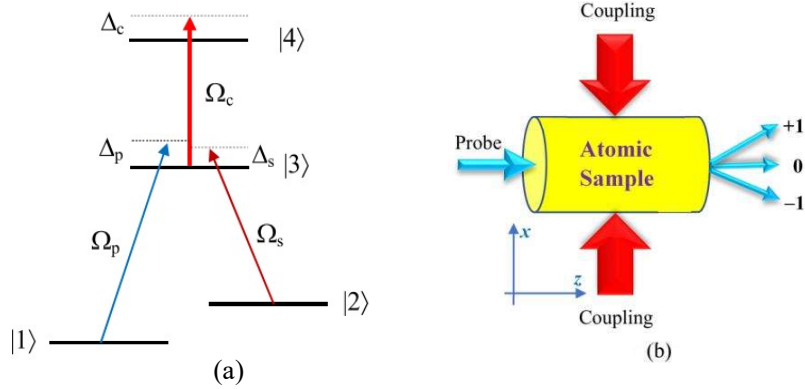


Fig. 1. (a) Four-level inverted-Y atomic system. (b) Orientations of probe and coupling laser fields propagating through the atomic sample.

In the framework of the semiclassical theory, using the dipole and rotating wave approximations, the evolution of system can be represented by the following density matrix equations:

$$\dot{\rho}_{23} = \frac{i}{2}\Omega_s(\rho_{33} - \rho_{22}) - \frac{i}{2}\Omega_p\rho_{21} - \frac{i}{2}\Omega_c\rho_{24} + [-i\Delta_s - \gamma_{32}]\rho_{23}, \quad (1)$$

$$\dot{\rho}_{24} = \frac{i}{2}\Omega_s\rho_{34} - \frac{i}{2}\Omega_c\rho_{23} + [-i(\Delta_s + \Delta_c) - \gamma_{42}]\rho_{24}, \quad (2)$$

$$\dot{\rho}_{34} = -\frac{i}{2}(\Omega_p\rho_{14} + \Omega_s\rho_{24}) + \frac{i}{2}\Omega_c(\rho_{44} - \rho_{43}) + [-i\Delta_s - \gamma_{43}]\rho_{34}, \quad (3)$$

$$\dot{\rho}_{21} = -\frac{i}{2}\Omega_p\rho_{23} + \frac{i}{2}\Omega_s\rho_{31} + [i(\Delta_p - \Delta_s) - \gamma_{21}]\rho_{21}, \quad (4)$$

$$\dot{\rho}_{31} = -\frac{i}{2}\Omega_p(\rho_{33} - \rho_{11}) + \frac{i}{2}\Omega_s\rho_{21} + \frac{i}{2}\Omega_c\rho_{41} + [i\Delta_p - \gamma_{31}]\rho_{31}, \quad (5)$$

$$\dot{\rho}_{41} = -\frac{i}{2}\Omega_p\rho_{43} + \frac{i}{2}\Omega_c\rho_{31} + [i(\Delta_p + \Delta_c) - \gamma_{41}]\rho_{41}, \quad (6)$$

where, $\Omega_p = d_{31}E_p/\hbar$, $\Omega_c = d_{42}E_c/\hbar$ and $\Omega_s = d_{32}E_s/\hbar$ are Rabi frequency for the probe, coupling and signal fields, respectively; d_{kl} is element of dipole moment of the $|k\rangle \rightarrow |l\rangle$ transition and γ_{kl} is the decay rate of the atomic coherence ρ_{kl} , and Γ_{kl} is the decay rate of population from level $|k\rangle$ to level $|l\rangle$. The frequency detuning of the coupling, probe and signal light beams is respectively defined as $\Delta_c = \omega_c - \omega_{43}$, $\Delta_p = \omega_p - \omega_{31}$ and $\Delta_s = \omega_s - \omega_{32}$.

Now we solve the density-matrix equations under the steady-state condition to find the solutions for density matrix elements related to the probe and signal responses up to third order. Under the assumption that the coupling light intensity Ω_c is much stronger than the probe light intensity Ω_p and signal light intensity Ω_s , therefore from Eqs. (1)-(6) we obtain:

$$\rho_{31} = \frac{-i\Omega_p / 2}{\left[(i\Delta_p - \gamma_{31}) + \frac{\Omega_s^2 / 4}{[i\Delta_p - i\Delta_s - \gamma_{21}]} + \frac{\Omega_c^2 / 4}{[i\Delta_p + i\Delta_c - \gamma_{41}]} \right]} . \quad (7)$$

When the coupling laser field is in the form of a standing wave along the x -direction (see Fig. 1b), the coupling Rabi frequency can be expressed as $\Omega_c = \Omega_{c0} \sin(\pi x / \Lambda)$, with $\Lambda = \frac{\lambda_c}{2 \sin \phi}$, λ_c is the wavelength of the coupling field, the angle ϕ is made by the direction of the coupling field to the direction of the probe field, and Λ is the spatial frequency of the standing wave.

The susceptibility of the atomic medium for the probe field is calculated by:

$$\chi_{31} = -\frac{Nd_{31}}{\varepsilon_0 E_p} \rho_{31} , \quad (8)$$

with N is the atomic density.

From Eq. (8) we obtain the normalized transmission function of probe field for the effective length L of the medium as:

$$T(x) = e^{-\text{Im}(\chi_{31})L} e^{i\text{Re}(\chi_{31})L} . \quad (9)$$

where, the terms $e^{-\text{Im}(\chi_{31})L}$ and $e^{i\text{Re}(\chi_{31})L}$ are associated with absorption and phase modulations of the grating, respectively. The Fraunhofer diffraction pattern of the probe field can be obtained by the Fourier transform of the transmission function $T(x)$, as follows:

$$I_p(\theta) = |F(\theta)|^2 \cdot \frac{\sin^2(M\pi \sin(\theta)R)}{M^2 \sin^2(\pi \sin(\theta)R)} . \quad (10)$$

$$F(\theta) = \int_0^1 T(x) \exp(-2i\pi x \cdot \sin(\theta)R) dx , \quad (11)$$

where θ is the diffraction angle of the probe field associated with the z -direction, $R = \Lambda/\lambda_p$, and M is the parameter that characterizes the spatial width of the probe field.

III. RESULTS AND DISCUSSION

We apply to the ^{87}Rb atom with two ground levels $|1\rangle$ and $|2\rangle$ are assigned to the states $5S_{1/2}$, $F = 1$ and $F = 2$, respectively, while the states $|3\rangle$ and $|4\rangle$ are chosen as $5P_{3/2}$, $F' = 1$ and $5D_{5/2}$, $F'' = 1$, respectively. The atomic parameters are given by: $N = 10^{12}$ atoms/cm³, $\Gamma_{32} = \Gamma_{42} = 0.97\text{MHz}$, $\Gamma_{31} = \Gamma_{32} = 6\text{MHz}$, $d_{31} = 1.6 \times 10^{-29}$ C.m, $d_{32} = 1.6 \times 10^{-29}$ C.m, $\omega_p = 3.77 \times 10^8$ MHz.

In Fig. 2, we demonstrate the formation of a diffraction pattern of the probe field in the standing wave coupling field and no the signal field. The diffraction pattern includes zero-, first- and second-order diffractions. When the coupling intensity is increased, the intensity of zero-order diffraction increases, and higher orders decrease.

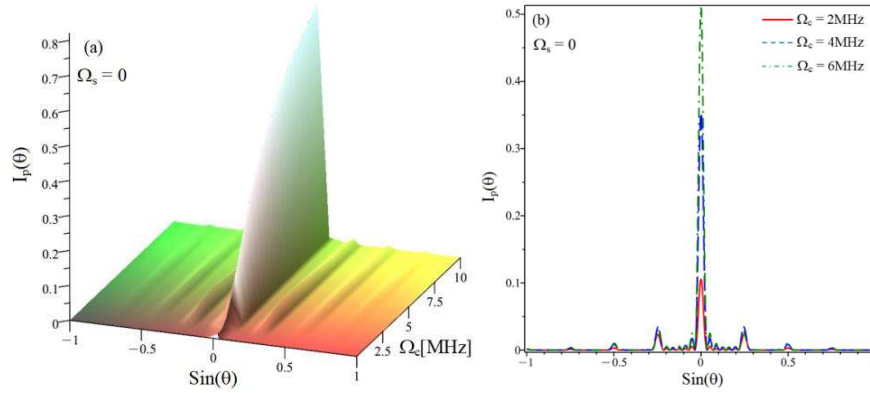


Fig. 2. The diffraction pattern of the probe field versus coupling laser when $\Omega_s = 0$ and $\Delta_c = 0$.

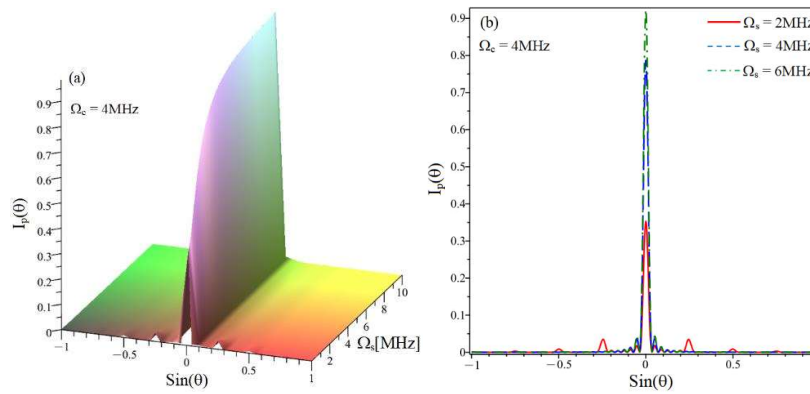


Fig. 3. The diffraction pattern of the probe field versus signal laser when $\Omega_c = 4\text{MHz}$, $\Delta_c = 0$.

Fig. 3 shows the dependence of the diffraction pattern on the signal laser intensity (Ω_s). Also, when the signal intensity is increased, the intensity of zero-order diffraction increases while higher orders decrease.

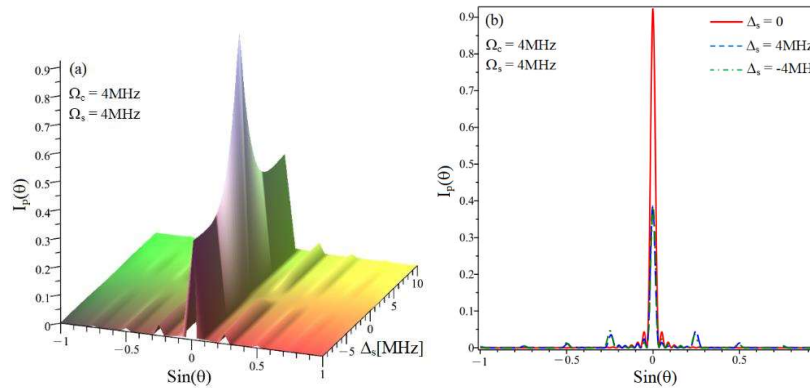


Fig. 4. The diffraction pattern of the probe field versus signal detuning when $\Omega_c = \Omega_s = 4\text{MHz}$ and $\Delta_c = 0$.

Fig. 4 shows the dependence of the diffraction pattern on the signal frequency detuning Δ_s . By tuning the signal frequency, the energy of the probe field is transferred from zero-order diffraction to first-order diffraction.

Finally, Fig. 5 displays the dependence of the diffraction pattern on the coupling frequency detuning Δ_c . Also, when changing the coupling frequency, the energy of the probe field is also transferred from zero-order diffraction to first-order diffraction.

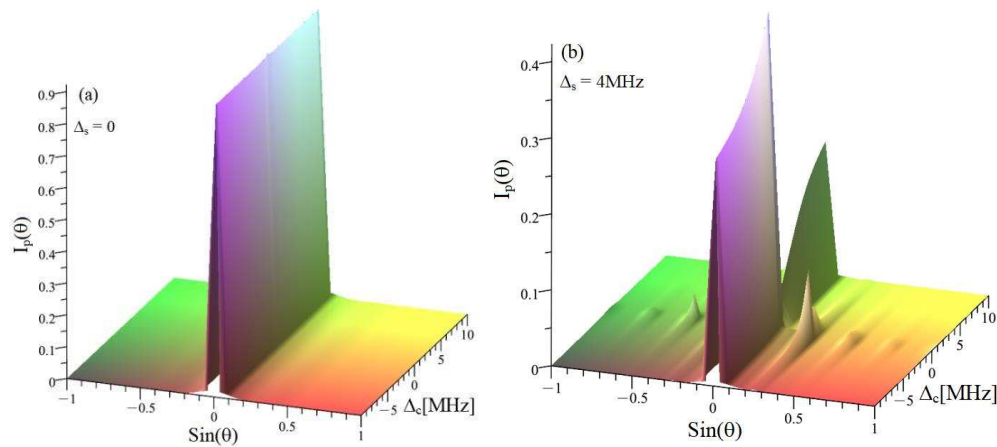


Fig. 5. The diffraction pattern of the probe field versus coupling detuning when $\Omega_s = \Omega_c = 4\text{MHz}$, $\Delta_s = 0$ (a) and $\Delta_s = 4\text{MHz}$ (b).

IV. CONCLUSION

Probe diffraction grating has created in the four-level inverted-Y atomic medium placed in the standing wave coupling field. In the presence of signal laser field, the light energy switching between the zero-, first-, and second-order diffractions can be achieved by tuning frequency and/or intensity of the coupling and signal fields.

ACKNOWLEDGEMENTS. This research was funded by Vingroup Innovation Foundation (VINIF) under project code VINIF.2022.DA00076 and Vietnam's Ministry of Education and Training under Grant No. B2023-TDV-08.

REFERENCES

- [1] N. Bonod, J. Neauport, *Adv. Opt. Photon.*, **8**, 2016, pp. 156-199.
- [2] K. J. Boller, A. Imamoglu, S.E. Harris, *Phys. Rev. Lett.*, **66**, 1991, pp. 2593.
- [3] N. H. Bang, L. V. Doai and D. X Khoa, *Comm. Phys.*, **28**, 2019, pp. 1-33.
- [4] M. Mitsunaga and N. Imoto, *Phys. Rev. A*, **59**, 1999, pp. 4773-4776.
- [5] S. A. Carvalho and L. E. E. de Araujo, *Phys. Rev. A*, **83**, 2011, pp. 053825.
- [6] S. Asghar, Ziauddin, S. Qamar, and S. Qamar, *Phys. Rev. A*, **94**, 2016, pp. 033823.
- [7] T. Naseri, *Physics Letters A*, **384**, 2020, pp. 126164.
- [8] T. Qiu and G. Yang, *J. Phys. B: At. Mol. Opt. Phys.*, **48**, 2015, pp. 245502.
- [9] Gh. Solookinejad, et al., , *Chin. J. Phys.*, **54**, 2016, pp. 651-658.
- [10] R. Sadighi-Bonabi, T. Naseri, and M. Navadeh-Toupchi, *App. Opt.*, **54**, 2015, pp. 368-377.
- [11] N. Ba, et al., *Opt. Commun.*, **285**, 2012, pp. 3792-3797.
- [12] Hussain, M. Abbas, H.T. Ali, *Phys. Scr.*, **96**, 2021, pp. 125110.